

Moment-Based Parametric Identification of Arrays of Wave Energy Converters*

Yerai Peña-Sanchez[†], Nicolás Faedo[†] and John V. Ringwood[†]

Abstract—The motion of a Wave Energy Converter (WEC) can be described in terms of an integro-differential equation, which includes a convolution term accounting for the radiation forces. Since such a convolution term represents a drawback for both simulation and model-based control, it is usually approximated by a parametric form to be later embedded into the WEC dynamical equation. When an array of WECs is considered, a separate convolution term is required for each cross-coupling component (arising from device interactions), which increases the complexity of the problem. In this paper, a framework to compute a parametric model for array of WEC devices based on moment-matching is presented. The proposed method shows a significant simulation computational saving, compared to other parametric identification methods, which is illustrated by the means of a numerical example.

I. INTRODUCTION

Among the different renewable energy sources, wave energy has one of the highest power densities [1]. However, the cost involved in generating power from waves is still prohibitive, compared to wind or solar [1]. At this development stage, modelling accurate but simple dynamical models is crucial for both the optimization of the different components of a Wave Energy Converters (WECs), and the development of control strategies that maximise power conversion.

Boundary Element Methods (BEMs), such as NEMOH [2], are the most commonly used methods to calculate the hydrodynamic parameters of WECs, due to their low computational complexity [3]. Nevertheless, the coefficients are computed in the frequency-domain, characterising only the steady-state motion of the device under analysis. This represents a drawback for control strategies, which require of a time-domain representation of the WEC motion.

The motion of a floating device can be expressed in the time-domain in terms of the well-known Cummins' equation [4], whose parameters can be computed from the frequency-domain hydrodynamic coefficients obtained by BEM solvers. The resulting time-domain formulation is an integro-differential equation which contains a convolution term accounting for the radiation forces acting on the device. Such a convolution term represents a drawback both for simulation, since its highly computationally inefficient to compute, and for control strategies, which often require of a state-space representation of the system dynamics. To avoid such issues, this convolution term is usually approximated by a finite-order parametric model (expressed in terms of a

state-space approximation) for which several strategies can be found in the literature such as [5].

We note that the majority of the literature only considers the single-input single-output (SISO) WEC case. However, since commercial WECs are likely to be deployed in arrays to minimise costs [6], the computation of multiple-input multiple-output (MIMO) parametric models becomes of paramount importance (see, for example, [7]). Such MIMO WEC systems require an impulse response function for each cross-coupling component (arising from inter-device interactions), raising the total number of convolution operations to N^2 , where N is the number of devices. Furthermore, the usual approach in the literature is to compute a parametric form (of order n_r) for each of these cross-coupling subsystems, leading to an input-output system of order $2N + n_r N^2$. Though computationally more efficient than solving N^2 convolutions, the final dimension of the model still increases exponentially with N , which can render a global control technique intractable for real-time applications [8].

To address such an issue, this paper proposes an extension of the SISO moment-matching based identification framework, developed in [5], for MIMO systems. Moment-matching methods interpolate a certain number of points on the complex plane, which are directly related to the frequency-response of the target dynamical system. In fact, the transfer function of the approximated model *exactly* matches the steady-state behaviour of the target system at these specific interpolation points, which can be used to ensure the reliability of the approximated model at the most (dynamically) relevant frequencies such as, for example, the resonant frequency of the device. The method proposed herein allows for the computation of fully parametric WEC array models, easing the application of real-time control/estimation techniques, which is crucial to maximise the energy extracted by a given WEC and, therefore, for the economic viability of wave energy [6].

The remainder of this paper is organised as follows. Section II recalls key concepts behind the moment-matching framework for both SISO and MIMO systems. Section III presents the dynamics of a WEC array, while Section IV presents a moment-based analysis of such a system. Section V proposes the moment-matching-based methodology to compute finite-order parametric models for the force-to-motion dynamics of the array. Finally, Section VI deals with an application case, with Section VII briefly presenting conclusions.

*This material is based upon works supported by Science Foundation Ireland under Grant no. 13/IA/1886.

[†]Yerai Peña-Sanchez, Nicolás Faedo and John V. Ringwood are with the Centre for Ocean Energy Research, Maynooth University, Maynooth, Ireland yerai.pena.2017@mumail.ie

A. Notation and Preliminaries

Standard notation is considered through this study, with any exceptions detailed in this section. \mathbb{C}^0 denotes the set of pure-imaginary complex numbers and \mathbb{C}^- denotes the set of complex numbers with a negative real part. The symbol 0 stands for any zero element, dimensioned according to the context. The symbol \mathbb{I}_n denotes an order n identity matrix. The spectrum of a matrix $A \in \mathbb{R}^{n \times n}$, i.e. the set of its eigenvalues, is denoted as $\lambda(A)$. The notation W^\dagger , with $W \in \mathbb{R}^{n \times m}$, denotes the *Moore-Penrose* inverse of W . The symbol \bigoplus denotes the direct sum of n matrices, i.e. $\bigoplus_{i=1}^n A_i = \text{diag}(A_1, A_2, \dots, A_n)$. The expression $\|X\|_F$ denotes the *Frobenius* norm of the matrix X . The *Kronecker product* between two matrices $M_1 \in \mathbb{R}^{n \times m}$ and $M_2 \in \mathbb{R}^{p \times q}$ is denoted as $M_1 \otimes M_2 \in \mathbb{R}^{np \times mq}$, while the *Kronecker delta* function is denoted as δ_{ij} . The convolution between two functions $f(t)$ and $g(t)$ over a finite range $[0, t]$, i.e. $\int_0^t f(\tau)g(t-\tau)d\tau$ is denoted as $f * g$. The Fourier transform of a function $f(t) \in L^2(\mathbb{R})$ is denoted by $\hat{f}(j\omega)$. The symbol $e_{ij}^q \in \mathbb{R}^{q \times q}$ denotes a matrix with 1 in the ij component and 0 elsewhere. Finally, the symbol $\varepsilon_n \in \mathbb{R}^{n \times 1}$ denotes a vector with odd components equal to 1 and even components equal to 0. In the remainder of this section, the formal definitions of two important operators are presented, since their definition in the literature can often be ambiguous.

Definition 1: [9] (*Kronecker sum*) The *Kronecker sum* between two matrices P_1 and P_2 , with $P_1 \in \mathbb{R}^{n \times n}$ and $P_2 \in \mathbb{R}^{k \times k}$, is defined (and denoted) as

$$P_1 \hat{\oplus} P_2 \triangleq P_1 \otimes \mathbb{I}_k + \mathbb{I}_n \otimes P_2. \quad (1)$$

Definition 2: [9] (*Vec operator*) Given a matrix $P = [p_1, p_2, \dots, p_m] \in \mathbb{R}^{n \times m}$, where $p_j \in \mathbb{R}^n$, $j = 1, \dots, m$, the vector valued operator *vec* is defined as

$$\text{vec}\{P\} \triangleq [p_1^\top \quad p_2^\top \quad \dots \quad p_m^\top]^\top \in \mathbb{R}^{nm}. \quad (2)$$

II. MODEL ORDER REDUCTION BY MOMENT-MATCHING

A. Moments for SISO systems

Consider a finite-dimensional, SISO, continuous-time system described, for $t \geq 0$, by the state-space model

$$\dot{x}(t) = Ax(t) + Bu(t), \quad y(t) = Cx(t), \quad (3)$$

where $x(t) \in \mathbb{R}^n$, $u(t) \in \mathbb{R}$, $y(t) \in \mathbb{R}$, $A \in \mathbb{R}^{n \times n}$, $B \in \mathbb{R}^n$ and $C \in \mathbb{R}^{1 \times n}$. Consider the associated transfer function $W(s) = C(s\mathbb{I}_n - A)^{-1}B : \mathbb{C} \rightarrow \mathbb{C}$ and assume that (3) is minimal (i.e. controllable and observable).

Definition 3: [10] The 0-moment of system (3) at $s_i \in \mathbb{C} \setminus \lambda(A)$ is the complex number $\eta_0(s_i) = C(s_i\mathbb{I}_n - A)^{-1}B$. The k -moment of system (3) at $s_i \in \mathbb{C}$ is the complex number

$$\eta_k(s_i) = \frac{(-1)^k}{k!} \left[\frac{d^k}{ds^k} W(s) \right]_{s=s_i}, \quad (4)$$

with $k \geq 1$ integer.

Remark 1: The idea of the moment-based model order reduction technique is based on interpolating the transfer function of the original system (and the derivatives of this)

and the transfer function of the reduced order model (and the derivatives of this) at these interpolation points s_i .

In [11] it is shown that the moments of system (3) are in a one-to-one relation with the steady-state response (provided it exists) of the output of the interconnection between a signal generator and system (3), as recalled in the following.

Theorem 1: [11] Consider system (3) and the autonomous signal generator

$$\dot{\xi}(t) = S\xi(t), \quad u(t) = L\xi(t), \quad (5)$$

with $\xi(t) \in \mathbb{R}^\nu$, $S \in \mathbb{R}^{\nu \times \nu}$, $L \in \mathbb{R}^{1 \times \nu}$ and $\xi(0) \in \mathbb{R}^\nu$. Assume that the triple $(L, S, \xi(0))$ is minimal, $\lambda(A) \subset \mathbb{C}^-$, $\lambda(S) \subset \mathbb{C}^0$ and the eigenvalues of S are simple. Let $\Pi \in \mathbb{R}^{n \times \nu}$ be the (unique) solution of the Sylvester equation

$$A\Pi + BL = \Pi S. \quad (6)$$

Then, there exists a one-to-one relation between the moments $\eta_0(s_1), \eta_0(s_2), \dots, \eta_0(s_\nu)$, with $s_i \in \lambda(S)$ for all $i = 1, \dots, \nu$, and the steady-state response $C\Pi\xi$ of the output y of the interconnection of system (3) with the signal generator (5). In fact, the moments are uniquely determined by the matrix $C\Pi$.

Remark 2: The minimality of the triple $(L, S, \xi(0))$ implies the observability of the pair (L, S) and the *excitability*¹ of the pair $(S, \xi(0))$.

Remark 3: From now on, we refer to the matrix $C\Pi \equiv \bar{Y}$ as the moment-domain equivalent of $y(t)$.

B. MIMO case

Consider a finite-dimensional, MIMO, continuous-time system described, for $t \geq 0$, by the state-space model

$$\dot{x}(t) = Ax(t) + Bu(t), \quad y(t) = Cx(t), \quad (7)$$

with $x(t) \in \mathbb{R}^n$, $u(t) \in \mathbb{R}^q$, $y(t) \in \mathbb{R}^q$, $A \in \mathbb{R}^{n \times n}$, $B \in \mathbb{R}^{n \times q}$ and $C \in \mathbb{R}^{q \times n}$. Consider the associated transfer function $W(s) = C(s\mathbb{I}_n - A)^{-1}B : \mathbb{C} \rightarrow \mathbb{C}^{q \times q}$ and assume that (7) is minimal. We now recall an adaptation of Theorem 1 for the MIMO case².

Theorem 2: [14] Consider system (7) and the autonomous multiple-output signal generator

$$\dot{\Xi}(t) = (\mathbb{I}_q \otimes S)\Xi(t), \quad u(t) = L\Xi(t), \quad (8)$$

with $\Xi(t) \in \mathbb{R}^{q\nu}$, $L \in \mathbb{R}^{q \times q\nu}$, $\Xi(0) \in \mathbb{R}^{q\nu}$, S as in Theorem 1 and assume that the triple of matrices $(L, \mathbb{I}_q \otimes S, \Xi(0))$ is minimal. Let $\Pi \in \mathbb{R}^{n \times q\nu}$ be the (unique) solution of the Sylvester equation

$$A\Pi + BL = \Pi(\mathbb{I}_q \otimes S). \quad (9)$$

As for Theorem 1, there exists a one-to-one relation between the moments $\eta_0(s_1), \eta_0(s_2), \dots, \eta_0(s_\nu)$, with $s_i \in \lambda(S)$ for all $i = 1, \dots, \nu$, and the steady-state response $C\Pi\Xi$ of the

¹We refer the reader to [12] for the definition of excitability.

²We note that the literature in moment-matching for the MIMO case utilises the so-called *tangential interpolation* framework [13]. Herein, we are interested in retaining the exact same steady-state response for the WEC array, in despite of the consequently increase in model order.

output y of the interconnection of system (7) with the signal generator (8).

Based on this steady-state interpretation of moments, we recall the following definition, adapted for the MIMO case.

Definition 4: [11] Consider the signal generator (8). The system described by the equations

$$\dot{\Theta}(t) = F\Theta(t) + Gu(t), \quad \theta(t) = Q\Theta(t), \quad (10)$$

with $\Theta \in \mathbb{R}^{q\nu}$, $\theta(t) \in \mathbb{R}^q$, $F \in \mathbb{R}^{q\nu \times q\nu}$, $G \in \mathbb{R}^{q\nu \times q}$ and $Q \in \mathbb{R}^{q \times q\nu}$ is a model of system (7) at S if system (10) has the same moments at S as system (7).

Lemma 1: [11] Consider system (7) and the signal generator (8). Then, the system (10) is a model of system (7) at S if³ $\lambda(F) \cap \lambda(S) = \emptyset$ and

$$\bar{Y} = QP, \quad (11)$$

where $\bar{Y} = C\Pi$ is the moment-domain equivalent of the output of system (7) computed from (9) and P is the unique solution of the Sylvester equation

$$FP + GL = P(\mathbb{I}_q \otimes S). \quad (12)$$

Remark 4: The steady-state output of the reduced order model (10) exactly matches the steady-state output of the system resulting from the interconnection of system (7) and the signal generator (8).

III. WEC ARRAY EQUATIONS OF MOTION

The linearised equation of motion for an array of N wave energy converters can be expressed in the time-domain according to Newton's second law, obtaining the following linear hydrodynamic formulation:

$$M\ddot{\chi}(t) = \mathcal{F}_r(t) + \mathcal{F}_h(t) + \mathcal{F}_e(t), \quad (13)$$

where $M = \bigoplus_{i=1}^N m_i$ is the mass matrix of the buoy with m_i the mass of the i -th device, and the elements of the vectors $\chi, \mathcal{F}_e, \mathcal{F}_h, \mathcal{F}_r \in \mathbb{R}^N$ contain the excursion $x_i(t)$, excitation force $f_{e_i}(t)$ (external input), hydrostatic restoring force $f_{h_i}(t)$, and radiation force $f_{r_i}(t)$ acting on the i -th device ($i \in \{1, \dots, N\}$) of the array, respectively.

The linearised hydrostatic force $\mathcal{F}_h(t)$ can be written as $-S_h\chi(t)$, where $S_h = \bigoplus_{i=1}^N s_{h_i}$ and each $s_{h_i} > 0$ denotes the hydrostatic stiffness of the i -th WEC. The radiation force $\mathcal{F}_r(t)$ is modelled from linear potential theory and, using Cummins' equation [4], is

$$\mathcal{F}_r(t) = -\mu_\infty \ddot{\chi}(t) - \int_0^t K(\tau) \dot{\chi}(t - \tau) d\tau, \quad (14)$$

where $\mu_\infty = \lim_{\omega \rightarrow +\infty} A(\omega)$, $\mu_\infty > 0$ represents the added-mass matrix at infinite frequency [15] and $K(t) = \sum_{i=1}^N \sum_{j=1}^N e_{ij}^N \otimes k_{ij}(t) \in \mathbb{R}^{N \times N}$, $k_{ij}(t) \in L^2(\mathbb{R})$ contains the (causal) radiation impulse response of each device (if $i = j$) and each interaction due to the radiated waves created by the motion of other devices (if $i \neq j$).

Thus, Eq. (13) can be rewritten as

$$(M + \mu_\infty) \ddot{\chi}(t) + K(t) * \dot{\chi}(t) + S_h \chi(t) = \mathcal{F}_e(t), \quad (15)$$

³Note that $\lambda(\mathbb{I} \otimes A) = \lambda(A)$ for any matrix $A \in \mathbb{R}^{n \times n}$ [9].

whose internal stability has been analysed and guaranteed for any physically meaningful values of the parameters and the mapping $K(t)$ [15]. Note that, in the general case, a control force input $u(t)$ (which is supplied by the so-called *power take-off* system [16]) can be straightforwardly incorporated in (15), though this does not have any implications in the method proposed herein and, hence, it is not considered in the upcoming sections. Regarding the WEC energy conversion process, the interested reader is referred to [16] for further detail.

Given that BEM solvers compute the frequency response of the device under analysis, we represent the motion of the WEC array using a frequency-domain description. Considering the velocity of each device as measurable outputs i.e. $\dot{\chi}(t)$, the following representation

$$\hat{\chi}(j\omega) = \hat{\mathcal{F}}_e(j\omega)H(j\omega), \quad (16)$$

where $H : \mathbb{C}^0 \rightarrow \mathbb{C}^{N \times N}$ denotes the force-to-velocity frequency response mapping of the WEC array, holds. $H(j\omega)$ can be computed as a function of a well-known set of frequency-dependent parameters, [15] namely

$$H(j\omega) = \left(B(\omega) + j\omega(A(\omega) + M) + \frac{S_h}{j\omega} \right)^{-1}, \quad (17)$$

where $B(\omega)$ and $A(\omega)$ represent the radiation damping, and the radiation added mass matrix of the device, respectively. These parameters are calculated using hydrodynamic codes at a finite set of uniformly spaced frequency samples $\Omega = \{\omega_i\}_{i=1}^M$ with $\Omega \subset [\omega_l, \omega_u]$ where ω_l and ω_u represents the lower and upper bound of the range, respectively⁴.

IV. MOMENT-BASED WEC ARRAY FORMULATION

We present the motion equation of (15) in a structure more suited to the theoretical results documented in Section II. The following state-space representation, for the WEC array dynamics, is proposed:

$$\dot{\varphi}(t) = A_\varphi \varphi(t) + B_\varphi u(t), \quad y_\varphi(t) = C_\varphi \varphi(t) = \dot{\chi}(t), \quad (18)$$

where $\varphi(t) = [\phi_1, \dots, \phi_N]^\top \in \mathbb{R}^{2N}$ is the state-vector of the continuous-time model, with $\phi_i = [x_i(t), \dot{x}_i(t)]^\top$. The function $u(t) \in \mathbb{R}^N$, assumed to be the input of system (18), is defined as

$$u(t) = \mathcal{F}_e(t) - K(t) * \dot{\chi}(t), \quad (19)$$

Under this assumption, the matrices in (18) can be written in compact form as follows:

$$A_\varphi = \sum_{i=1}^N \sum_{j=1}^N e_{ij}^N \otimes A_{\varphi_{ij}}, \quad B_\varphi = \sum_{i=1}^N \sum_{j=1}^N e_{ij}^N \otimes B_{\varphi_{ij}}, \quad (20)$$

$$C_\varphi = \mathbb{I}_N \otimes [0 \ 1],$$

⁴We note that, though the target frequency-domain data $H(j\omega)$ is virtually always computed using BEM codes, these data points can be provided by means of, for example, experimental testing.

with each $A_{\varphi_{ij}} \in \mathbb{R}^{2 \times 2}$, $B_{\varphi_{ij}} \in \mathbb{R}^2$ defined as

$$A_{\varphi_{ij}} = \begin{bmatrix} 0 & i_j \delta \\ -\mathcal{M}_{ij} s_{h_i} & 0 \end{bmatrix}, \quad B_{\varphi_{ij}} = \begin{bmatrix} 0 \\ \mathcal{M}_{ij} \end{bmatrix}, \quad (21)$$

where \mathcal{M}_{ij} is the ij -th element of the inverse generalised mass matrix $\mathcal{M} = (M + \mu_\infty)^{-1}$.

The excitation force (input) vector is expressed as an autonomous multiple-output implicit form signal generator as

$$\dot{\Xi}_e(t) = (\mathbb{I}_N \otimes S) \Xi_e(t), \quad \mathcal{F}_e(t) = L_e \Xi_e(t), \quad (22)$$

where the dimension of S is as in (5), $\Xi_e(t) \in \mathbb{R}^{N\nu}$, $L_e \in \mathbb{R}^{N \times N\nu}$ and, without loss of generality, the initial condition of the signal generator is chosen as $\Xi_e(0) = \varepsilon_{N\nu}$. Given the characteristics of $\lambda(S)$, we consider the finite set $\mathcal{F} = \{\omega_p\}_{p=1}^f \subset \mathbb{R}$ and write the matrix S in a real block-diagonal form as

$$S = \bigoplus_{p=1}^f S_p, \quad S_p = \begin{bmatrix} 0 & \omega_p \\ -\omega_p & 0 \end{bmatrix}, \quad (23)$$

where $\nu = 2f$, $f \geq 0$ integer. Note that, with this selection of matrices, the assumption on the minimality of the triple $(L_e, \mathbb{I}_N \otimes S, \Xi_e(0))$ holds as long as the pair $(L_e, \mathbb{I}_N \otimes S)$ is observable.

Remark 5: Note that each ω_p in (23) represents a desired interpolation point for the model reduction process, i.e. a frequency where the transfer function of the reduced order model matches the transfer function of the original system. Under this selection of matrices, the moments of system (18), driven by the signal generator (22), can be computed by solving a specific Sylvester equation (see Theorem 2) which, for the WEC array case, can be expressed as

$$A_\varphi \Pi_\varphi + B_\varphi (L_e - \bar{\mathcal{Z}}) = \Pi_\varphi (\mathbb{I}_N \otimes S), \quad (24)$$

where $\Pi_\varphi \in \mathbb{R}^{2N \times N\nu}$ and $\bar{\mathcal{Z}}$ is the moment-domain equivalent of the radiation matrix convolution term. The moment-domain equivalent of the velocity can be expressed in terms of the solution of (24) straightforwardly as $\bar{\mathcal{V}} = C_\varphi \Pi_\varphi$. The following lemma allows for the explicit computation of $\bar{\mathcal{Z}}$ in terms of Π_φ .

Lemma 2: [14] The moment-domain equivalent of the convolution integral in (14) can be computed as

$$\bar{\mathcal{Z}} = \sum_{i=1}^N \sum_{j=1}^N e_{ij}^N \bar{\mathcal{V}} (\mathbb{I}_N \otimes \mathcal{R}_{ij}), \quad (25)$$

where each $\mathcal{R}_{ij} \in \mathbb{R}^{\nu \times \nu}$ is a block-diagonal matrix defined by

$$\mathcal{R}_{ij} = \bigoplus_{p=1}^f \begin{bmatrix} i_j r_{\omega_p} & i_j m_{\omega_p} \\ -i_j m_{\omega_p} & i_j r_{\omega_p} \end{bmatrix}, \quad (26)$$

and its entries depend on the ij -th element of the added mass matrix $A(\omega)_{ij}$ and the radiation damping matrix $B(\omega)_{ij}$ of the device at each specific frequency induced by the eigenvalues of S , as

$$i_j r_{\omega_p} = B(\omega_p)_{ij}, \quad i_j m_{\omega_p} = \omega_p [A(\omega_p)_{ij} - \mu_{\infty ij}], \quad (27)$$

where $\mu_{\infty ij}$ is the ij -th element of the matrix μ_∞ .

With the analytical definition of the moment-domain equivalent of the radiation force convolution term in (25), we are now ready to recall the following lemma, that addresses the explicit computation of the moment equivalent $\bar{\mathcal{V}}$.

Lemma 3: [14] Under the internal stability assumption of (15), the moment-domain equivalent of the output y_φ of system (18) can be uniquely determined as

$$\text{vec}\{\bar{\mathcal{V}}\} = (\mathbb{I}_N \otimes \Phi_\varphi^{\mathcal{R}}) \text{vec}\{L_e\} \quad (28)$$

where

$$\begin{aligned} \Phi_\varphi^{\mathcal{R}} &= (\mathbb{I}_\nu \otimes C_\varphi) \Phi_\varphi^{-1} (\mathbb{I}_\nu \otimes B_\varphi), \\ \Phi_\varphi &= (S \hat{\oplus} A_\varphi) + \sum_{i=1}^N \sum_{j=1}^N \mathcal{R}_{ij}^T \otimes -B_\varphi e_{ij}^N C_\varphi. \end{aligned} \quad (29)$$

with $\Phi_\varphi \in \mathbb{R}^{2N\nu \times 2N\nu}$ and $\Phi_\varphi^{\mathcal{R}} \in \mathbb{R}^{N\nu \times N\nu}$.

Lemma 3 explicitly shows how to compute the moment-domain equivalent of the output of system (18), i.e. the velocities of the WEC array. We use this result in Section V, to compute moment-matching-based time-domain models that *exactly* match the steady-state response of the target array at each of the frequencies defined by the user in the matrix S .

V. MODELS ACHIEVING MOMENT-MATCHING

This section proposes a systematic method to compute an approximated time-domain model of the input-output dynamics of the WEC array, based on the moment-domain representation of the N -devices WEC array dynamics derived in Section IV. We regard these moment-based concepts in synergy with some results of subspace-based identification methods as proposed in [17].

Under the subspace-based strategy developed in [17], both the dynamic and output matrix from system (18) can be approximated in terms of the singular value decomposition of the Hankel matrix, constructed from the input-output frequency-domain data of the WEC array (17). This α -dimensional approximated matrices ${}^d\hat{A}_\alpha \in \mathbb{R}^{\alpha \times \alpha}$, $\hat{C}_\alpha \in \mathbb{R}^{N \times \alpha}$ (where ${}^d\hat{A}_\alpha$ corresponds to a discrete-time model) can be computed⁵ as

$${}^d\hat{A}_\alpha = (J_1 \hat{U}_\alpha)^\dagger J_2 \hat{U}_\alpha, \quad \hat{C}_\alpha = J_3 \hat{U}_\alpha. \quad (30)$$

where the continuous-time equivalent matrix \hat{A}_α can be obtained directly from ${}^d\hat{A}_\alpha$ using, for instance, the bilinear transformation.

We propose a method that exploits the result of Lemma 3 and the system structure of (10), which can be summarised in the following steps:

- 1) Select a set of f interpolation points (frequencies) $\mathcal{F} = \{\omega_p\}_{p=1}^f$ to achieve moment-matching.
- 2) Compute the matrix $\mathbb{I}_N \otimes S$ following (23) and select any L_e such that the pair $(L_e, \mathbb{I}_N \otimes S)$ is observable.

⁵We refer the reader to [17] for the explicit expression of the matrices J_1, J_2, J_3 and \hat{U} .

- 3) Calculate the moment-domain equivalent of the output of system (18) \bar{V} using the result of Lemma 3.
- 4) Compute the matrices $\hat{A}_{N\nu}$ and $\hat{C}_{N\nu}$ from (30).
- 5) Consider the model of (10) and set $F = F_\varphi = \hat{A}_{N\nu}$ and $Q = Q_\varphi = \hat{C}_{N\nu}$.
- 6) Consider the frequency response of (10) as a function of the input matrix G_φ i.e.

$$\tilde{H}(j\omega, G_\varphi) = Q_\varphi(j\omega_i - F_\varphi)^{-1} G_\varphi$$

Using the frequency set $\Omega = \{\omega_i\}_{i=1}^M$, compute G_φ^{opt} with the following optimisation-based procedure:

$$G_\varphi^{\text{opt}} = \arg \min_{G_\varphi} \sum_{i=1}^M \left\| \tilde{H}(j\omega_i, G_\varphi) - H(j\omega_i) \right\|_F^2$$

subject to:

$$F_\varphi P_\varphi + G_\varphi L_e = P_\varphi (\mathbb{I}_N \otimes S), \quad Q_\varphi P_\varphi = \bar{V}.$$

- 7) Compute a $N\nu$ -dimensional WEC array time-domain model achieving moment-matching at S as

$$\tilde{\mathcal{H}}_{\mathcal{F}} : \begin{cases} \dot{\Theta}_\varphi(t) &= F_\varphi \Theta_\varphi(t) + G_\varphi^{\text{opt}} \mathcal{F}_e(t), \\ \theta_\varphi(t) &= Q_\varphi \Theta_\varphi(t). \end{cases}$$

The method is based on the idea of building the model $\tilde{\mathcal{H}}_{\mathcal{F}}$ by matching the f (user defined) frequencies of the set \mathcal{F} , exploiting the system structure of (10), and solving for an equality-constrained optimisation problem, which computes the input matrix G_φ^{opt} that minimises the difference between the target frequency response and that of (10), while ensuring the moment-matching conditions in the model. The proposed optimisation formulation is a constrained least squares problem and can be solved using computationally efficient state-of-the-art solvers.

VI. APPLICATION CASE

This section presents an application case to illustrate the proposed strategy. Specifically, the array system is composed of four identical spherical heaving bodies constrained to move in heave, arranged in a square layout (as in Fig. 1) with an inter-device spacing of $d = 20$ [m]. Each spherical body has a diameter of 10 [m], a draft of 5 [m] and a mass of 4×10^5 [kg]. For the numerical examples of this section, the irregular waves are described by a JONSWAP spectrum [18] with a peak period of $T_p = 6$ [s], significant wave height $H_s = 1.5$ [m] and peak enhancement factor $\gamma = 3.3$.

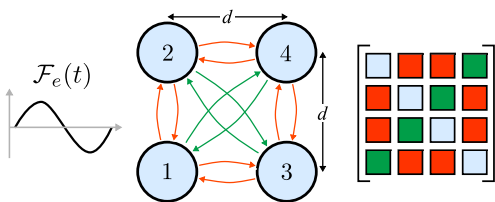


Fig. 1. WEC array layout considered (adapted from [7]). The colour of the arrows represent different interactions, while the colored box at the right represents the position of each interaction in the MIMO system.

From now on, we refer to the frequency-domain model of the WEC array (17) as the *target* (or benchmark) re-

sponse. For the sake of comparison, in the case of time-domain simulations, the results obtained by the parametric models computed using the framework proposed in this study are compared to the ones obtained using Cummins' equation (Eq. (15)) both directly, where the radiation force is computed by explicitly solving the convolution terms, and considering a state-space approximation of order (for this case) $n_r = 6$. In Table I, we refer to these two models as *Full conv.* and *Conv. SS*, respectively. In order to get meaningful results for this time-domain scenario, and since the waves are generated from sets of random amplitudes, it is found that the mean of 10 simulations is necessary to obtain a 95% confidence interval with a half-width of 0.25% of the mean, computed as in [7].

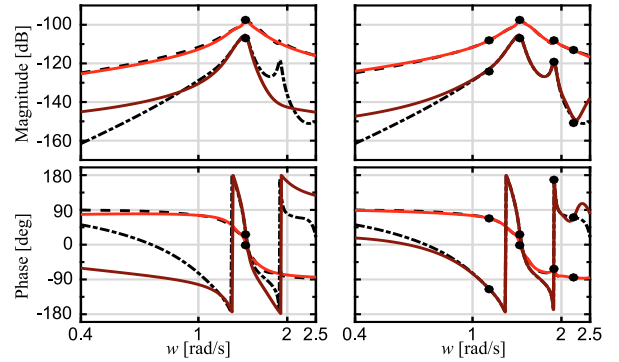


Fig. 2. Frequency response of the inner-dynamics of body 1 $\{1, 1\}$ (target in dashed-black, approximated in solid-red) and the interaction between bodies 1 and 4 $\{1, 4\}$ (target in dash-dotted-black, approximated in solid-brown). The left plots correspond to $\tilde{\mathcal{H}}_{\mathcal{F}_1}$, while the right plots correspond to $\tilde{\mathcal{H}}_{\mathcal{F}_4}$. The black dots represent the (user-selected) interpolation frequencies.

Fig. 2 presents the target frequency response of the WEC array $H(j\omega)$ computed from (17), along with the frequency response of the models $\tilde{\mathcal{H}}_{\mathcal{F}_1}$ and $\tilde{\mathcal{H}}_{\mathcal{F}_4}$. Particularly, Fig. 2 presents the Bode diagram for the elements $\{1, 1\}$ (the inner dynamics of body 1) and $\{1, 4\}$ (interaction between bodies 1 and 4) of the corresponding transfer function matrix. As already reported for the SISO case in [5], the selection of the set \mathcal{F} has to be done in a (dynamically) sensible manner. For $\tilde{\mathcal{H}}_{\mathcal{F}_1}$, as shown in Fig. 2, the interpolation point is chosen as the frequency where the maximum amplitude peak occurs in the target frequency response (1.45 [rad/s]). For the case of $\tilde{\mathcal{H}}_{\mathcal{F}_4}$, the set of frequencies \mathcal{F}_4 naturally includes \mathcal{F}_1 , and increases the number of interpolation points by adding the frequency where the second peak occurs (1.89 [rad/s]), along with lower and higher frequency components. The approximation error decrease from $\tilde{\mathcal{H}}_{\mathcal{F}_1}$ to $\tilde{\mathcal{H}}_{\mathcal{F}_4}$ can be appreciated directly from Fig. 2, or more precisely from Table I.

We note that there is a significant difference in terms of the magnitude between the target frequency response diagonal element $\{1, 1\}$ (inner-dynamics) and the off-diagonal element $\{1, 4\}$ (interaction-dynamics) depicted in Fig. 2, which is accentuated outside the range where both amplitude peaks occur. That said, even though the approximation of $\tilde{\mathcal{H}}_{\mathcal{F}_1}$, in the case of the element $\{1, 4\}$, seems to be poor, the

model is able to capture the most significant dynamics as a consequence of a sensible choice of the interpolation point.

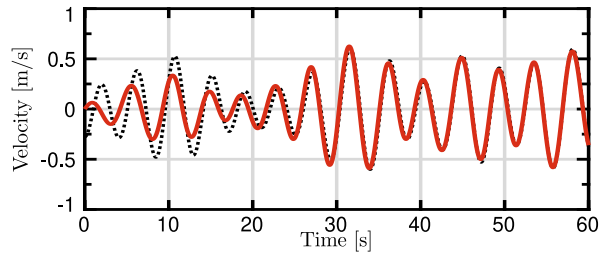


Fig. 3. Comparison between the time-domain output (velocity) of device number 1 for $\tilde{\mathcal{H}}_{\mathcal{F}_4}$ (solid-red) and its the steady-state response computed from $H(j\omega)$ (dotted-black).

Fig. 3 shows the time-domain response of $\tilde{\mathcal{H}}_{\mathcal{F}_4}$ for an irregular wave input. It can be appreciated that, in steady-state, the approximated model (solid-red) coincides with the motion results obtained from the target model (dotted-black).

Table I offers a numerical appraisal of each of the computed models for the case of device motion simulation in terms of the following characteristics:

Dim Dimension of the parametric model.

NRMSE_F Normalized Root Mean Square Error (NRMSE) computed against the target WEC array frequency responses for $\omega \in [0.3, 2.5]$.

NRMSE_T NRMSE computed against the target steady-state responses averaged over 10 different simulations.

N-Time The time required⁶ for the time-domain simulation normalized against the fastest model.

TABLE I
COMPARISON TABLE.

Model	Dim	NRMSE _F	NRMSE _T	N-Time
Full conv.	∞	0	0	941.83
Conv. SS	104	0.2007	0.0998	2.3670
$\tilde{\mathcal{H}}_{\mathcal{F}_1}$	8	0.2391	0.1043	1
$\tilde{\mathcal{H}}_{\mathcal{F}_2}$	16	0.0914	0.0658	1.0070
$\tilde{\mathcal{H}}_{\mathcal{F}_3}$	24	0.0552	0.0233	1.0581
$\tilde{\mathcal{H}}_{\mathcal{F}_4}$	32	0.0383	0.0126	1.0951

It should be highlighted that, as discussed in Section I, when considering a parametric form for each of the radiation force subsystems (*Conv. SS*), the dimension of the model increases exponentially with N , while it increases linearly ($2fN$) with the proposed strategy. Additionally, the dynamics of the radiation force subsystem are usually more complex than the input-output dynamics of device, often requiring a higher order approximation to successfully capture its relevant features. Therefore, as can be appreciated from Table I, the model *Conv. SS* of dimension 104 obtains similar force-to-motion results to those computed by $\tilde{\mathcal{H}}_{\mathcal{F}_1}$ with only 8 elements in its state-space representation, and in less than half of the computational time.

⁶Measured using the MATLAB embedded functions `Tic` and `Toc`.

VII. CONCLUSIONS

This paper introduces a strategy to obtain a MIMO finite-order parametric model of WEC array systems using raw frequency-domain data computed by BEM solvers, based on recent advances on model order reduction by moment-matching. This strategy exactly matches the target frequency-response at a set of user-selected frequencies. Furthermore, the proposed framework allows for the computation of an accurate low dimensional approximation, compared to the methods employed in the wave energy array literature.

ACKNOWLEDGEMENT

The authors are sincerely grateful to Prof. Alessandro Astolfi and Dr. Giordano Scarciotti from Imperial College London, for useful discussions on the moment-based theory. This material is based upon works supported by Science Foundation Ireland under Grant no. 13/IA/1886.

REFERENCES

- [1] J. Cruz, *Ocean wave energy: current status and future perspectives*. Springer Science & Business Media, 2008.
- [2] A. Babarit and G. Delhommeau, "Theoretical and numerical aspects of the open source BEM solver NEMOH," in *11th European Wave and Tidal Energy Conference, Nantes*, 2015.
- [3] M. Penalba, T. Kelly, and J. V. Ringwood, "Using nemoh for modelling wave energy converters: A comparative study with wamit," 2017.
- [4] W. Cummins, "The impulse response function and ship motions," DTIC Document, Tech. Rep., 1962.
- [5] N. Faedo, Y. Peña-Sanchez, and J. V. Ringwood, "Finite-order hydrodynamic model determination for wave energy applications using moment-matching," *Ocean Engineering*, vol. 163, pp. 251 – 263, 2018.
- [6] K. Ruehl and D. Bull, "Wave Energy Development Roadmap: Design to commercialization," *OCEANS 2012 MTS/IEEE: Harnessing the Power of the Ocean*, 2012.
- [7] Y. Peña-Sanchez, M. Garcia-Abril, F. Paparella, and J. V. Ringwood, "Estimation and forecasting of excitation force for arrays of wave energy devices," *IEEE Transactions on Sustainable Energy*, 2018.
- [8] N. Faedo, S. Olaya, and J. V. Ringwood, "Optimal control, MPC and MPC-like algorithms for wave energy systems: An overview," *IFAC Journal of Systems and Control*, 2017.
- [9] J. Brewer, "Kronecker products and matrix calculus in system theory," *IEEE Transactions on circuits and systems*, vol. 25, no. 9, pp. 772–781, 1978.
- [10] A. C. Antoulas, *Approximation of large-scale dynamical systems*. SIAM, 2005.
- [11] A. Astolfi, "Model reduction by moment matching for linear and nonlinear systems," *IEEE Transactions on Automatic Control*, vol. 55, no. 10, pp. 2321–2336, 2010.
- [12] A. Padoan, G. Scarciotti, and A. Astolfi, "A geometric characterization of the persistence of excitation condition for the solutions of autonomous systems," *IEEE Transactions on Automatic Control*, vol. 62, no. 11, pp. 5666–5677, 2017.
- [13] G. Scarciotti, "Low computational complexity model reduction of power systems with preservation of physical characteristics," *IEEE Transactions on Power Systems*, vol. 32, no. 1, pp. 743–752, 2017.
- [14] N. Faedo, G. Scarciotti, A. Astolfi, and J. V. Ringwood, "Moment-based constrained optimal control of an array of wave energy converters," in *American Control Conference (ACC), US (Accepted)*, 2019.
- [15] J. Falnes, *Ocean waves and oscillating systems: linear interactions including wave-energy extraction*. Cambridge university press, 2002.
- [16] N. Faedo, S. Olaya, and J. V. Ringwood, "Optimal control, mpc and mpc-like algorithms for wave energy systems: An overview," *IFAC Journal of Systems and Control (Peer-Review)*, vol. 1, 2017.
- [17] T. McKelvey, H. Akçay, and L. Ljung, "Subspace-based multivariable system identification from frequency response data," *IEEE Transactions on Automatic Control*, vol. 41, no. 7, pp. 960–979, 1996.
- [18] K. Hasselmann, "Measurements of wind wave growth and swell decay during the Joint North Sea Wave Project (JONSWAP)," *Dtsch. Hydrogr. Z.*, vol. 8, p. 95, 1973.